Magn Reson Med Sci 2021; 20; 396–403
doi:10.2463/mrms.mp.2020-0103
Published Online: February 9, 2021

MAJOR PAPER

Triexponential Diffusion Analysis of Diffusion-weighted Imaging for Breast Ductal Carcinoma *in Situ* and Invasive Ductal Carcinoma

Masako Ohno[1†], Naoki Ohno[2†], Tosiaki Miyati[2*], Hiroko Kawashima[2,3], Kazuto Kozaka[3], Yukihiro Matsuura[1], Toshifumi Gabata[3], and Satoshi Kobayashi[1,2,3]

Purpose: To obtain detailed information in breast ductal carcinoma *in situ* (DCIS) and invasive ductal carcinoma (IDC) using triexponential diffusion analysis.

Methods: Diffusion-weighted images (DWI) of the breast were obtained using single-shot diffusion echo-planar imaging with 15 b-values. Mean signal intensities at each b-value were measured in the DCIS and IDC lesions and fitted with the triexponential function based on a two-step approach: slow-restricted diffusion coefficient (D_s) was initially determined using a monoexponential function with b-values > 800 s/mm^2. The diffusion coefficient of free water at 37°C was assigned to the fast-free diffusion coefficient (D_f). Finally, the perfusion-related diffusion coefficient (D_p) was derived using all the b-values. Furthermore, biexponential analysis was performed to obtain the perfusion-related diffusion coefficient (D^*) and the perfusion-independent diffusion coefficient (D). Monoexponential analysis was performed to obtain the apparent diffusion coefficient (ADC). The sensitivity and specificity of the aforementioned diffusion coefficients for distinguishing between DCIS and IDC were evaluated using the pathological results.

Results: The D_s, D, and ADC of DCIS were significantly higher than those of IDC ($P < 0.01$ for all). There was no significant correlation between D_p and D_s, but there was a weak correlation between D^* and D. The combination of D_p and D_s showed higher sensitivity and specificity (85.9% and 71.4%, respectively), compared to the combination of D^* and D (81.5% and 33.3%, respectively).

Conclusion: Triexponential analysis can provide detailed diffusion information for breast tumors that can be used to differentiate between DCIS and IDC.

Keywords: *breast tumor, diffusion-weighted imaging, intravoxel incoherent motion, triexponential diffusion analysis*

Introduction

MRI is an important diagnostic tool for the detection and characterization of breast lesions. The primary purposes of the breast MRI are to a) detect breast tumors and b) evaluate the extent of the tumor.[1–3] Differentiation among various malignant breast tumor types, such as ductal carcinoma *in situ* (DCIS) and invasive ductal carcinoma (IDC), is essential for patient treatment and management.[4,5] Breast tumors can be classified by evaluating signal intensity changes in T_1-weighted dynamic contrast-enhanced MRI (DCE-MRI).[6] However, there are several cases in which differentiating among various tumor types using DCE-MRI alone may be difficult given the overlapping features that lead to false-positive findings.[7–9] Despite its variable specificity (75%–98%), DCE-MRI has shown high sensitivity for the diagnosis of breast lesions.[10]

Diffusion-weighted imaging (DWI) has been extensively applied to the various body organs and to the central nervous system. DWI of the breast has potential clinical applicability considering evidence showing that specificity can be improved by evaluating the apparent diffusion coefficient (ADC) calculated from DWI as an adjunct technique to DCE-MRI.[11–13] Many

[1]Department of Radiological Technology, Kanazawa University Hospital, Kanazawa, Ishikawa, Japan
[2]Faculty of Health Sciences, Institute of Medical, Pharmaceutical and Health Sciences, Kanazawa University, Kanazawa, Ishikawa, Japan
[3]Department of Radiology, Kanazawa University Hospital, Kanazawa, Ishikawa, Japan
[†]The authors equally contributed to this work.
*Corresponding author: Faculty of Health Sciences, Institute of Medical, Pharmaceutical and Health Sciences, Kanazawa University, 5-11-80, Kodatsuno, Kanazawa, Ishikawa 920-0942, Japan. E-mail: ramiyati@mhs.mp.kanazawa-u.ac.jp

Received: July 1, 2020 | Accepted: November 13, 2020

studies have reported differences in the *ADC* between benign and malignant breast tumors.[14–20] Although these observations may be explained by the highly restricted diffusion of water molecules in the malignant tumors owing to the higher cellularity compared with normal tissue and benign tumors, the exact mechanisms have not been fully clarified yet. A previous study showed that *ADC* decreases with increasing b-values in normal mammary glands and malignant breast tumors,[21] suggesting that the *ADC*, assuming monoexponential signal decay on DWI, depends on the b-values used and includes multiple biological data from the tissues, such as perfusion and cellularity.

Multi-exponential signal decay in DWI has been reported to be caused by various physiological processes and factors, such as perfusion, intra- and extracellular diffusions, and the permeability of blood vessels and cell membranes.[14,19,22,23] Le Bihan et al. reported that biexponential signal attenuation, including the effects from perfusion and diffusion, was observed in tissues when DWI was performed with the b-value range used in clinical settings.[24] The same authors first introduced intravoxel incoherent motion (IVIM) analysis with a biexponential function to provide both perfusion and diffusion information. The usefulness of IVIM analysis has been reported in various organs, such as the brain, liver, kidney, breast, and prostate.[25–35] Other studies have demonstrated that fast and slow diffusion components exist in the brain and result in a biexponential decay on DWI acquired over an extended range of b-values.[22,29,36] Hayashi et al.[37] evaluated the diffusion coefficients of three components, i.e., perfusion-related diffusion, fast-free diffusion, and slow-restricted diffusion (respectively, denoted by D_p, D_f, and D_s), using triexponential analysis of DWI data with multiple b-values in normal and liver cirrhosis cases. They successfully demonstrated the usefulness of triexponential analysis for the diagnosis of liver cirrhosis. Nakagawa et al.[38] first performed triexponential analysis of breast images in IDC and fibroadenoma (FA), and showed that a) the D_p in IDC was significantly higher than in FA, and b) the D_s was significantly lower than FA. These results are mainly attributed to the abundant perfusion and high cellularity in malignant tumors, and suggest that it is possible to differentiate between benign and malignant breast tumors with triexponential analysis. We, therefore, hypothesized that a more accurate differentiation of DCIS from IDC using triexponential analysis may be possible because it can provide more detailed information on perfusion and diffusion compared with bi- and monoexponential analyses. However, no prior report has compared the triexponential diffusion coefficients of DCIS with those of IDC.

Therefore, the current study evaluated three diffusion coefficients in DCIS and IDC using triexponential analysis and compared the results with bi- and monoexponential analyses.

Materials and Methods

Subjects

The institutional review board approved this retrospective study. Written informed consent requirement was waived considering the retrospective study. A total of 108 female patients with malignant breast lesions were included in the present study. All patients (age range, 31–82 years; mean, 56.7 years) underwent preoperative breast MRI at our institution, including DWI, from November 2012 to July 2014. None of the cases received neoadjuvant chemotherapy or hormonal therapy prior to MRI, and the tumors were surgically resected and pathologically evaluated. Consequently, the following pathological diagnoses were obtained: IDC (n = 66, age range = 31–82 years, mean = 56.1 years) and DCIS (n = 18, age range = 41–78 years, mean = 59.2 years). Mixed pathology cases (IDC and DCIS, n = 24) were excluded from the study. In our hospital, breast MRI was conducted without considering the menstrual cycle, even among premenopausal females.

Imaging conditions

All patients were examined on a 3.0 T MRI system (Signa HDxt; GE Healthcare, Milwaukee, WI, USA) equipped with an eight-channel breast phased array coil. For triexponential analysis, 2D single-shot spin echo diffusion echo-planar imaging with fat suppression was performed with the b-values of 0, 20, 40, 80, 120, 200, 400, 600, 800, 1000, 1200, 1500, 2000, 2500, and 3000 s/mm^2. The transverse DWI of the breast was obtained with the following parameters: TR, 5025 ms; TE, 89.2 ms; FOV, 360 × 360 mm; parallel imaging the array spatial sensitivity encoding technique (ASSET) factor, 2; acquisition matrix, 128 × 128; slice thickness, 6.0 mm; slice gap, 1.5 mm; number of slices, 17; number of excitations, 2; separate diffusion measures in three orthogonal directions; and acquisition time of 7 min and 14s. The diffusion time was held constant in all b-value scans. DWI covered the whole mammary glandular tissue.

Diffusion analysis

The diffusion-weighted images of the breast were analyzed retrospectively using the software Image J (version 1.40g; National Institutes of Health, Bethesda, MD, USA). Signal intensities were measured in ROIs on all the b-values images (Fig. 1). The ROIs were manually drawn in all lesions (one per patient) on the DWIs. They were chosen to be slightly smaller than the actual lesions to avoid partial volume effects attributed to the surrounding normal tissues. Care was taken to exclude necrotic or cystic areas in the tumor. This was achieved by choosing the ROIs with reference to the early phase of contrast-enhanced T_1-weighted and T_2-weighted images. The mean ROI size was 67.2 mm^2 (range, 7.9–462.8 mm^2) and 36.7 mm^2 (range, 7.9–106.8 mm^2) on IDC and DCIS, respectively.

D_p, D_f, D_s, and their corresponding fractions (denoted as F_p, F_f, and F_s, respectively) were calculated from the following triexponential fitting using the Levenberg–Marquardt algorithmml:

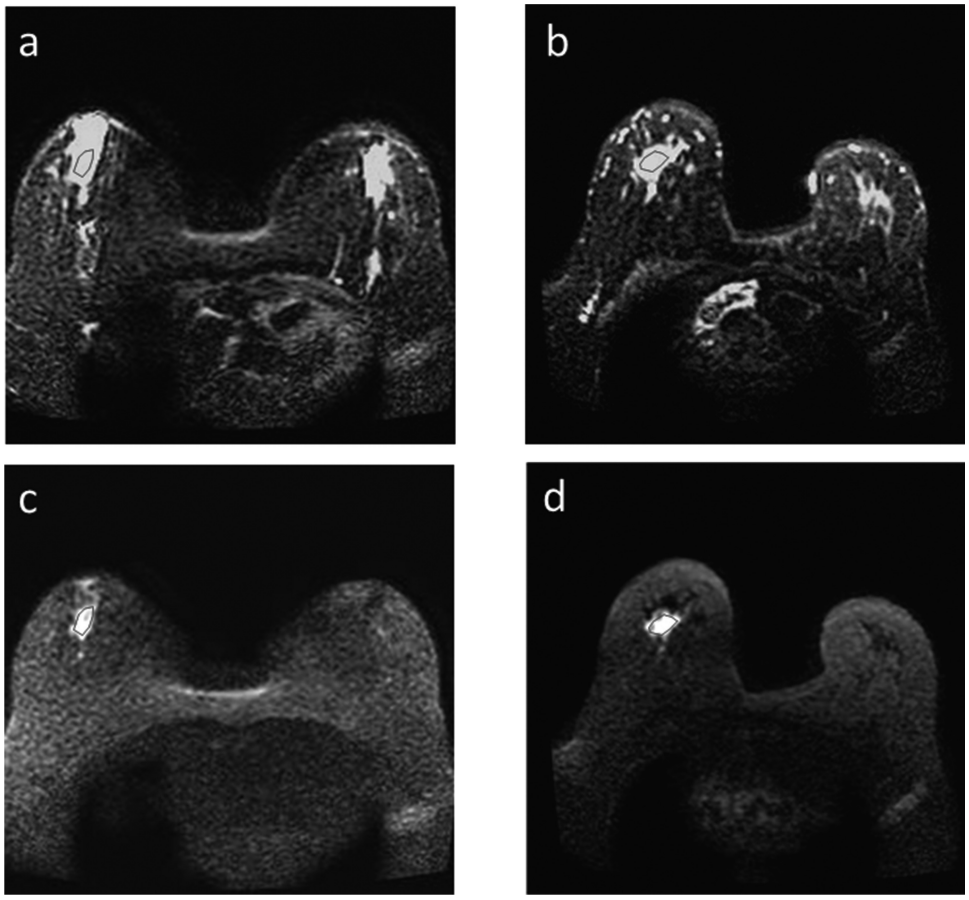

Fig. 1 Examples of region of interest setting on breast diffusion-weighted images with a b-value of (**a**, **b**) 0 and (**c**, **d**) 1500 s/mm^2 in (**a**, **c**) ductal carcinoma *in situ* and (**b**, **d**) invasive ductal carcinoma.

$$S_b/S_0 = F_p e(-bD_p) + F_f exp(-bD_f) + F_s exp(-bD_s) \quad [1]$$

where S_b and S_0 are signal intensities for a given b-value and for a b-value of 0 s/mm^2, respectively. To improve the fitting accuracy and robustness of the analysis, the fitting procedure was performed with a two-step approach.[39] The contribution of perfusion and free diffusion on the signal intensity can be negligible for b-values > 800 s/mm^2. Thus, D_s was first calculated for b-values > 800 s/mm^2 using the following equation (monoexponential function),

$$S_b/S_{int} = exp(-bD_s) \quad [2]$$

where S_{int} is the zero intercept at a b-value of 0 s/mm^2 in the first fitting procedure for b-values over 800 s/mm^2. Subsequently, D_s was applied to the triexponential function (Eq. [1]). In addition, the published value[40] of the diffusion coefficient of free water at 37°C (3.0×10^{-3} mm^2/s) was assigned to D_f. Using fixed D_s and D_f values, the D_p and F_p, F_f, and F_s, were determined for all b-values.

Moreover, bi- and monoexponential analyses were performed and compared with the triexponential analysis. We used a segmented approach for biexponential analysis. First, the perfusion-independent diffusion coefficient was calculated using the monoexponential function for b-values > 200 s/mm^2 because the contribution of perfusion on the signal intensity is quite small for b-values > 200 s/mm^2,[31,41]

$$S_b/S_{int} = exp(-bD) \quad [3]$$

where D is the perfusion-independent diffusion coefficient. Subsequently, D was applied to the following equation (biexponential function). By fixing the value of D, perfusion-related diffusion coefficient (D^*) and the fraction (F) were determined using all the b-values,

$$S_b/S_0 = Fexp(-bD^*) + (1-F)exp(-bD) \quad [4]$$

Monoexponential analysis was performed using the following equation (monoexponential function) with all b-values,

$$S_b/S_0 = exp(-b \cdot ADC) \quad [5]$$

where ADC is the apparent diffusion coefficient.

All fitting procedures were implemented and executed in MATLAB (version 2014a; MathWorks, Natick, MA, USA).

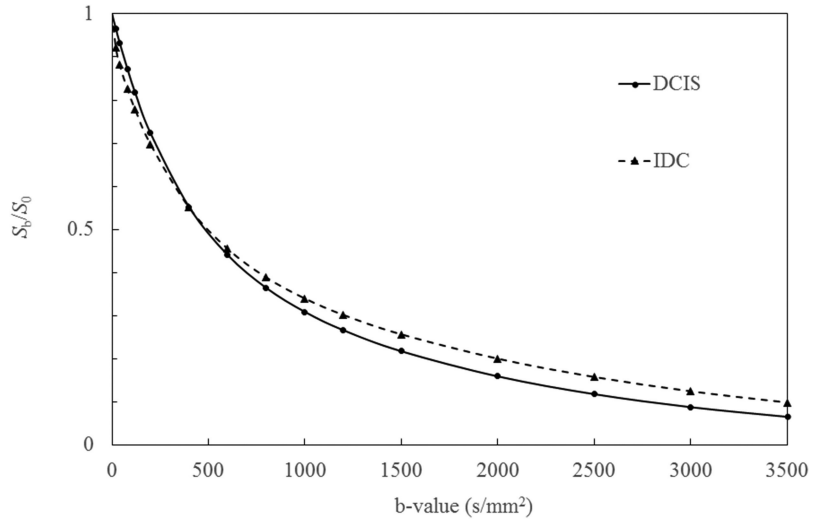

Fig. 2 Examples of triexponential signal intensity curves of diffusion-weighted images at each b-value in DCIS and IDC. DCIS, ductal carcinoma *in situ*; IDC, invasive ductal carcinoma.

Moreover, SNR measurement at the highest b-value (b = 3000 s/mm^2) was conducted to ensure that the SNR was high enough for accurate diffusion analysis. The SNR was calculated as a quotient of the mean signal intensity in the ROI inside the breast lesion and the standard deviation of the background noise near the lesion ROI.

statistical analyses

Statistical analyses were performed using SPSS for Windows (version 19.0; IBM, Armonk, NY, USA). Mann–Whitney U-test was used to compare the diffusion coefficients derived from tri-, bi-, and monoexponential analyses between DCIS and IDC. The relations between diffusion coefficients were evaluated using Spearman's correlation coefficient. A P value < 0.05 was considered statistically significant.

Receiver operating characteristic (ROC) analysis was conducted to evaluate the sensitivity and specificity of each diffusion coefficient for differentiating between DCIS and IDC. The optimal cutoff values were chosen using the maximum Youden index (i.e., sensitivity + specificity − 1). Additionally, logistic regression analysis was performed to derive models that distinguish between DCIS and IDC using the combination of diffusion coefficients (i.e., D_p and D_s or D^* and D).

Results

Examples of signal intensity curves for DCIS and IDC fitted by triexponential function are shown in Fig. 2. DCIS had a smaller signal intensity attenuation than IDC, especially at the lower b-values. By contrast, at the higher b-values, DCIS had greater signal attenuation than IDC.

The diffusion coefficients derived by tri-, bi-, and monoexponential analyses in DCIS and IDC are shown in Fig. 3 showing the corresponding box plots. D_s, D, and ADC of DCIS were significantly higher than those of IDC ($P < 0.01$ for all). No statistical difference in D_p and D^* was observed between DCIS and IDC ($P > 0.05$ for all). ROC analysis showed that the best cutoff values for D_p, D_s, D^*, D, and ADC to differentiate between DCIS and IDC were 3.02×10^{-3} mm^2/s (71.4% sensitivity and 40.4% specificity), 0.56×10^{-3} mm^2/s (64.3% sensitivity and 82.5% specificity), 4.89×10^{-3} mm^2/s (92.9% sensitivity and 40.4% specificity), 0.78×10^{-3} mm^2/s (71.4% sensitivity and 82.5% specificity), and 0.81×10^{-3} mm^2/s (92.9% sensitivity and 57.9% specificity), respectively. Logistic regression analysis showed a sensitivity and specificity of 85.9% and 71.4% for the combination of D_p and D_s and 81.5% and 33.3% for the combination of D^* and D, respectively.

Table 1 shows the relationships among all diffusion coefficients with tri-, bi-, and monoexponential analyses. There was no significant correlation between D_p and D_s, but there were weak positive correlations between D^* and D.

The mean SNRs at b = 3000 s/mm^2 were 12.37 ± 7.12 and 38.8 ± 31.7 for DCIS and IDC, respectively.

Discussion

In this study, we performed diffusion analyses of breast tumor DWI using tri-, bi-, and monoexponential functions, and compared the diffusion coefficients between DCIS and IDC.

The D_s estimated based on triexponential analysis was significantly higher in DCIS than in IDC. Sigmund et al. reported that the diffusion coefficient of the slow diffusion component obtained with biexponential analysis was dependent on tissue cellularity and was lower in malignant breast lesions than in normal fibroglandular tissue.[42] Therefore, we speculated that the D_s of the restricted diffusion component obtained with triexponential analysis also reflected the cellularity. A previous

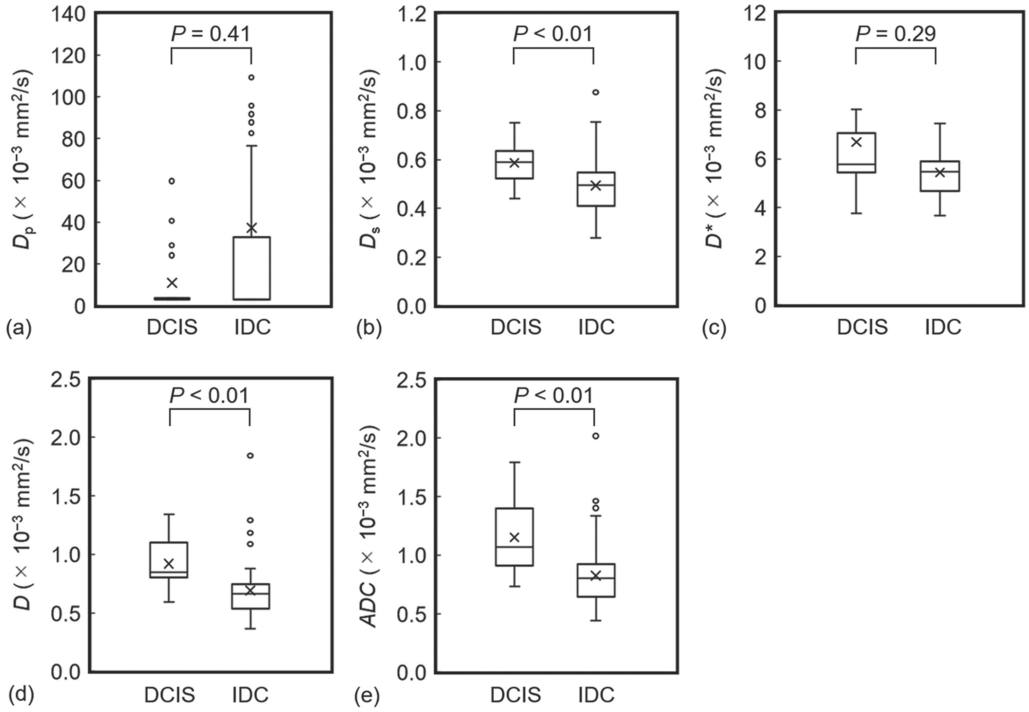

Fig. 3 Box plots of (**a**) D_p, (**b**) D_s, (**c**) D^*, (**d**) D, and (**e**) ADC in DCIS and IDC. For each group, the box plot illustrates the median (horizontal line inside box), mean (cross), and outlier (circle) values, interquartile range (box), and minimal and maximal values (lines extending above and below box). *ADC*, apparent diffusion coefficient; *D*, perfusion-independent diffusion coefficient; D^*, perfusion-related diffusion coefficient; DCIS, ductal carcinoma in situ; D_p, perfusionrelated diffusion coefficient; D_s, slow-restricted diffusion coefficient; IDC, invasive ductal carcinoma.

Table 1 Correlation coefficient (R) and *P* values between diffusion coefficients with tri-, bi-, and monoexponential analyses.

	D_p		D_s		D^*		D		ADC	
	R	*P*	R	*P*	R	*P*	R	*P*	R	*P*
D_p	NA	NA	0.088	0.467	0.795	0.001	0.095	0.430	0.212	0.076
D_s			NA	NA	0.278	0.019	0.910	0.001	0.85	0.001
D^*					NA	NA	0.252	0.034	0.347	0.003
D							NA	NA	0.98	0.001
ADC									NA	NA

ADC, apparent diffusion cofficient; *D*, perfusion-independent diffusion coefficient; D^*, perfusion-related diffusion coefficient; DCIS, ductal carcinoma in situ; D_p, perfusionrelated diffusion coefficient; D_s, slow-restricted diffusion coefficient; NA, not applicable.

study demonstrated lower cellularity in DCIS compared with high-grade IDC.[43] This explains our finding that DCIS had a higher D_s than IDC. Moreover, DCIS had a significantly larger *D* obtained with biexponential analysis and *ADC* obtained with monoexponential analysis than IDC. These results can be also explained by the difference in cellularity between DCIS and IDC.

The D_p obtained with triexponential analysis tended to be lower in DCIS than in IDC, although no significant difference was observed between both. Previous studies with triexponential analysis have demonstrated that D_p reflects perfusion in tissues.[37,39] In addition, Jensen et al.[1] reported that the signal enhancement in T_1-weighted images after contrast media administration was larger in mass lesions, including IDC, compared with non-mass lesions, including DCIS. Thus, the lower D_p in DCIS may be associated with the lower neovascularization compared with IDC.[44,45] However, the values exhibited large variabilities in both DCIS and IDC. This is likely responsible for the lack of a significant difference in D_p between DCIS and IDC, and can

be attributed to the physiological noise observed in lower b-values.[46] D_p variability should be mitigated by further optimization of imaging parameters and more robust fitting approaches, which need to be validated in future studies.

ROC and logistic regression analyses were performed to evaluate the diagnostic performance of the diffusion coefficients obtained from different diffusion models. Accordingly, our results found that *ADC* had the highest sensitivity, but limited specificity. Restricted diffusion and perfusion can affect *ADC* in opposite directions. Therefore, the confounding effect on *ADC* may be attributed to the lower specificity. Importantly, in terms of sensitivity and specificity, the combination of D_p and D_s with triexponential analysis outperformed the combination of D^* and D with biexponential analysis. These results suggest that triexponential diffusion analysis may have better diagnostic performance for differentiating between DCIS and IDC than biexponential diffusion analysis.

Although there was no significant correlation between D_p and D_s with triexponential analysis, D^* with biexponential analysis was weakly correlated with D. These findings indicate that the triexponential diffusion coefficients, i.e., D_p and D_s, do not necessarily represent the same type of information. Thus, the triexponential analysis could separate the effects of perfusion and diffusion in a better manner than biexponential analysis. Moreover, given that the same DWI data used for triexponential analysis can also be applicable to bi- and monoexponential analyses, the amount of information never decreases but rather increases.

The SNRs at the highest b-value (3000 s/mm^2) in both DCIS and IDC were sufficiently high for accurate estimation of diffusion coefficient (a SNR > 5 is needed).[39] However, we note that rigorous SNR measurements could not be used given that the use of parallel imaging introduces spatially varied noise, leading to position dependency of accuracy on SNR measurements.

There are several limitations associated with this study. First, we did not compare directly the D_s value in the tumor with cellularity. To clarify the relationship between them, the comparison between the D_s and the tumor cellularity obtained from the histopathological specimen should be pursued in the future. Second, the small number of DCIS cases resulted in an imbalanced number of subjects, which could potentially affect statistical results. Thus, further studies with a larger cohort are required. Third, the diffusion coefficients in the IDC case differed from those reported by Nakagawa et al.[38] The differences can be explained by the different b-values, fitting procedures, SNR, and MRI systems. Note that we used the modified triexponential fitting procedure, in which the D_f value was fixed to the diffusion coefficient of free water at 37°C to improve the accuracy and robustness of the analysis. This was because the original fitting reported in previous papers[37,38] induced considerable fitting errors, perhaps due to the large number of variables in the model and the relatively small blood volume in tissues. By contrast, previous reports[39,47] have shown that the modified fitting successfully demonstrated a strong correlation between D_p and cerebral blood flow derived by arterial spin labeling. We, therefore, considered that triexponential diffusion analysis with the modified fitting procedure would be suitable for extracting breast tumor perfusion information from DWI data. This choice could have presumably contributed to the observed differences in the diffusion coefficients. Further optimization of the fitting procedures and imaging parameters, including the b-values, is recommended to obtain more accurate and robust diffusion coefficients. Fourth, the fraction of diffusion components obtained with tri- and bi-exponential analyses was not evaluated given that the D_p values were approximated to D_f, especially in DCIS cases. In such cases, the corresponding fractions (F_p and F_f) do not make sense and, therefore, do not provide suitable physiological information. Moreover, previous studies have reported that several factors, such as blood volume, T_2 difference between blood and tissues, and noise contribution, can strongly affect the diffusion component fraction.[48–50] Thus, future studies need to consider more robust estimation and interpretation of the diffusion component fractions.

Conclusion

In conclusion, the D_s value that reflects restricted diffusion was significantly higher in DCIS than IDC. There was no correlation between D_p and D_s with triexponential analysis, while D^* and D with biexponential analysis exhibited a weak positive correlation. Triexponential diffusion analysis can provide more detailed information on perfusion and diffusion in breast tumors, and could thus assist in the differentiation between DCIS and IDC.

Conflicts of Interest

The authors declare that they have no conflict of interest.

References

1. Jensen LR, Garzon B, Heldahl MG, et al. Diffusion-weighted and dynamic contrast-enhanced MRI in evaluation of early treatment effects during neoadjuvant chemotherapy in breast cancer patients. J Magn Reson Imaging 2011; 34:1099–1109.
2. Kuhl CK, Schrading S, Bieling HB, et al. MRI for diagnosis of pure ductal carcinoma in situ: a prospective observational study. Lancet 2007; 370:485–492.
3. Liberman L, Morris EA, Dershaw DD, et al. Ductal enhancement on MR imaging of the breast. AJR Am J Roentgenol 2003; 181:519–525.
4. Jeevan R, Cromwell DA, Trivella M, et al. Reoperation rates after breast conserving surgery for breast cancer among women in England: retrospective study of hospital episode statistics. BMJ 2012; 345:e4505.

5. Chagpar AB, Killelea BK, Tsangaris TN, et al. A Randomized, Controlled Trial of Cavity Shave Margins in Breast Cancer. N Engl J Med 2015; 373:503–510.
6. Mann RM, Veltman J, Huisman H, et al. Comparison of enhancement characteristics between invasive lobular carcinoma and invasive ductal carcinoma. J Magn Reson Imaging 2011; 34:293–300.
7. Müller-Schimpfle M, Ohmenhaüser K, Stoll P, et al. Menstrual cycle and age: influence on parenchymal contrast medium enhancement in MR imaging of the breast. Radiology 1997; 203:145–149.
8. Delille JP, Slanetz PJ, Yeh ED, et al. Physiologic changes in breast magnetic resonance imaging during the menstrual cycle: perfusion imaging, signal enhancement, and influence of the T1 relaxation time of breast tissue. Breast J 2005; 11:236–241.
9. Kuhl CK, Bieling HB, Gieseke J, et al. Healthy premenopausal breast parenchyma in dynamic contrast-enhanced MR imaging of the breast: normal contrast medium enhancement and cyclical-phase dependency. Radiology 1997; 203:137–144.
10. Bogner W, Gruber S, Pinker K, et al. Diffusion-weighted MR for differentiation of breast lesions at 3.0 T: how does selection of diffusion protocols affect diagnosis?. Radiology 2009; 253:341–351.
11. Tsushima Y, Takahashi-Taketomi A, Endo K. Magnetic resonance (MR) differential diagnosis of breast tumors using apparent diffusion coefficient (ADC) on 1.5-T. J Magn Reson Imaging 2009; 30:249–255.
12. Chen X, Li WL, Zhang YL, et al. Meta-analysis of quantitative diffusion-weighted MR imaging in the differential diagnosis of breast lesions. BMC Cancer 2010; 10:693.
13. Partridge SC, DeMartini WB, Kurland BF, et al. Quantitative diffusion-weighted imaging as an adjunct to conventional breast MRI for improved positive predictive value. AJR Am J Roentgenol 2009; 193:1716–1722.
14. Sinha S, Lucas-Quesada FA, Sinha U, et al. In vivo diffusion-weighted MRI of the breast: potential for lesion characterization. J Magn Reson Imaging 2002; 15:693–704.
15. Ei Khouli RH, Jacobs MA, Mezban SD, et al. Diffusion-weighted imaging improves the diagnostic accuracy of conventional 3.0-T breast MR imaging. Radiology 2010; 256:64–73.
16. Kuroki-Suzuki S, Kuroki Y, Nasu K, et al. Detecting breast cancer with non-contrast MR imaging: combining diffusion-weighted and STIR imaging. Magn Reson Med Sci 2007; 6:21–27.
17. Hatakenaka M, Soeda H, Yabuuchi H, et al. Apparent diffusion coefficients of breast tumors: clinical application. Magn Reson Med Sci 2008; 7:23–29.
18. Marini C, Iacconi C, Giannelli M, et al. Quantitative diffusion-weighted MR imaging in the differential diagnosis of breast lesion. Eur Radiol 2007; 17:2646–2655.
19. Yankeelov TE, Lepage M, Chakravarthy A, et al. Integration of quantitative DCE-MRI and ADC mapping to monitor treatment response in human breast cancer: initial results. Magn Reson Imaging 2007; 25:1–13.
20. Wenkel E, Geppert C, Schulz-Wendtland R, et al. Diffusion weighted imaging in breast MRI: comparison of two different pulse sequences. Acad Radiol 2007; 14:1077–1083.
21. Takanaga M, Hayashi N, Miyati T, et al. [Influence of b value on the measurement of contrast and apparent diffusion coefficient in 3.0 Tesla breast magnetic resonance imaging]. Nihon Hoshasen Gijutsu Gakkai Zasshi 2012; 68:201–208. (in Japanese)
22. Schwarcz A, Bogner P, Meric P, et al. The existence of biexponential signal decay in magnetic resonance diffusion-weighted imaging appears to be independent of compartmentalization. Magn Reson Med 2004; 51:278–285.
23. Kiselev VG, Il'yasov KA. Is the "biexponential diffusion" biexponential?. Magn Reson Med 2007; 57:464–469.
24. Le Bihan D, Breton E, Lallemand D, et al. MR imaging of intravoxel incoherent motions: application to diffusion and perfusion in neurologic disorders. Radiology 1986; 161:401–407.
25. Maier SE, Bogner P, Bajzik G, et al. Normal brain and brain tumor: multicomponent apparent diffusion coefficient line scan imaging. Radiology 2001; 219:842–849.
26. Maier SE, Mulkern RV. Biexponential analysis of diffusion-related signal decay in normal human cortical and deep gray matter. Magn Reson Imaging 2008; 26:897–904.
27. Shinmoto H, Oshio K, Tanimoto A, et al. Biexponential apparent diffusion coefficients in prostate cancer. Magn Reson Imaging 2009; 27:355–359.
28. Tamura T, Usui S, Murakami S, et al. Biexponential Signal Attenuation Analysis of Diffusion-weighted Imaging of Breast. Magn Reson Med Sci 2010; 9:195–207.
29. Mulkern RV, Vajapeyam S, Robertson RL, et al. Biexponential apparent diffusion coefficient parametrization in adult vs newborn brain. Magn Reson Imaging 2001; 19:659–668.
30. Jia QJ, Zhang SX, Chen WB, et al. Initial experience of correlating parameters of intravoxel incoherent motion and dynamic contrast-enhanced magnetic resonance imaging at 3.0 T in nasopharyngeal carcinoma. Eur Radiol 2014; 24:3076–3087.
31. Liu C, Liang C, Liu Z, et al. Intravoxel incoherent motion (IVIM) in evaluation of breast lesions: comparison with conventional DWI. Eur J Radiol 2013; 82:e782-789.
32. Orton MR, Collins DJ, Koh DM, et al. Improved intravoxel incoherent motion analysis of diffusion weighted imaging by data driven Bayesian modeling. Magn Reson Med 2014; 71:411–420.
33. Tamura T, Usui S, Murakami S, et al. Comparisons of multi b-value DWI signal analysis with pathological specimen of breast cancer. Magn Reson Med 2012; 68:890–897.
34. Thoeny HC, Ross BD. Predicting and monitoring cancer treatment response with diffusion-weighted MRI. J Magn Reson Imaging 2010; 32:2–16.
35. Zhang JL, Sigmund EE, Rusinek H, et al. Optimization of b-value sampling for diffusion-weighted imaging of the kidney. Magn Reson Med 2012; 67:89–97.
36. Grinberg F, Farrher E, Kaffanke J, et al. Non-Gaussian diffusion in human brain tissue at high b-factors as examined by a combined diffusion kurtosis and biexponential diffusion tensor analysis. Neuroimage 2011; 57:1087–1102.
37. Hayashi T, Miyati T, Takahashi J, et al. Diffusion analysis with triexponential function in liver cirrhosis. J Magn Reson Imaging 2013; 38:148–153.
38. Nakagawa M, Miyati T, Hayashi T, et al. [Triexponential diffusion analysis in invasive ductal carcinoma and fibroadenoma].

Nihon Hoshasen Gijutsu Gakkai Zasshi 2014; 70:199–205. (in Japanese)
39. Ohno N, Miyati T, Kobayashi S, et al. Modified triexponential analysis of intravoxel incoherent motion for brain perfusion and diffusion. J Magn Reson Imaging 2016; 43:818–823.
40. Tofts PS, Jackson JS, Tozer DJ, et al. Imaging cadavers: cold FLAIR and noninvasive brain thermometry using CSF diffusion. Magn Reson Med 2008; 59:190–195.
41. Federau C, O'Brien K, Meuli R, et al. Measuring brain perfusion with intravoxel incoherent motion (IVIM): initial clinical experience. J Magn Reson Imaging 2014; 39:624–632.
42. Sigmund EE, Cho GY, Kim S, et al. Intravoxel incoherent motion imaging of tumor microenvironment in locally advanced breast cancer. Magn Reson Med 2011; 65:1437–1447.
43. Jiang R, Zeng X, Sun S, et al. Assessing detection, discrimination, and risk of breast cancer according to anisotropy parameters of diffusion tensor imaging. Med Sci Monit 2016; 22:1318–1328.
44. Bluff JE, Menakuru SR, Cross SS, et al. Angiogenesis is associated with the onset of hyperplasia in human ductal breast disease. Br J Cancer 2009; 101:666–672.
45. Adler EH, Sunkara JL, Patchefsky AS, et al. Predictors of disease progression in ductal carcinoma in situ of the breast and vascular patterns. Hum Pathol 2012; 43:550–556.
46. Rydhög AS, van Osch MJ, Lindgren E, et al. Intravoxel incoherent motion (IVIM) imaging at different magnetic field strengths: what is feasible?. Magn Reson Imaging 2014; 32:1247–1258.
47. Ohno N, Miyati T, Kobayashi S, et al. Reply to: On the perils of multiexponential fitting of diffusion MR data. J Magn Reson Imaging 2017; 45:1548.
48. Morvan D. In vivo measurement of diffusion and pseudo-diffusion in skeletal muscle at rest and after exercise. Magn Reson Imaging 1995; 13:193–199.
49. Jerome NP, d'Arcy JA, Feiweier T, et al. Extended T2-IVIM model for correction of TE dependence of pseudo-diffusion volume fraction in clinical diffusion-weighted magnetic resonance imaging. Phys Med Biol 2016; 61:N667-N680.
50. Neil JJ, Bretthorst GL. On the use of Bayesian probability theory for analysis of exponential decay data: an example taken from intravoxel incoherent motion experiments. Magn Reson Med 1993; 29:642–647.